Study of Low-Efficiency Droop in Semipolar ($20\bar{2}\bar{1}$) InGaN Light-Emitting Diodes by Time-Resolved Photoluminescence

Houqiang Fu, Zhijian Lu, Xin-Hao Zhao, Yong-Hang Zhang, *Fellow, IEEE*, Steven P. DenBaars, *Fellow, IEEE*, Shuji Nakamura, and Yuji Zhao

***Abstract*—The superior low-efficiency droop performance of semipolar ($20\bar{2}\bar{1}$) InGaN light-emitting diodes (LEDs) makes it a hot candidate for efficient solid-state lighting and full-color displays. To unveil the mystery of this low droop and high efficiency, the emission dynamics of semipolar ($20\bar{2}\bar{1}$) LEDs is investigated by time-resolved and steady-state photoluminescence (PL) measurements. Much smaller carrier lifetimes (radiative and nonradiative lifetime) were obtained from semipolar ($20\bar{2}\bar{1}$) InGaN QWs compared with those on the *c*-plane samples, possibly due to the reduced quantum-confined Stark effects and smaller indium fluctuation on semipolar InGaN samples. The experimental findings indicate a much reduced excess carrier density in semipolar ($20\bar{2}\bar{1}$) InGaN LEDs, which will impact the device performance. Based on this, a modified *ABC* equation with weak phase-space-filling (PSF) effect was used to model the droop characteristics of semipolar ($20\bar{2}\bar{1}$) LEDs.**

***Index Terms*—Efficiency droop, III-nitride, LEDs, semipolar.**

I. Introduction

III-nitride based light-emitting diodes (LEDs) have attracted considerable attention due to their wide applications in general lighting and displays [1]. Current commercial available InGaN LEDs grown on the conventional *c*-plane substrates, however, suffer from reduced efficiency with increasing current density, a notorious phenomenon known as "efficiency droop" [2]. Many different mechanisms have been proposed for the "efficiency droop" including carrier leakage [2], Auger recombination [3], [4], quantum confined Stark effect (QCSE) [5], carrier delocalization [6] and defects [7], while the physical origin is still being heavily debated [8]–[13]. *c*-plane LEDs usually have a quantum well (QW) thickness of 3 nm in order to mitigate the separation of electrons and holes. Zhao *et al.* developed staggered QW structure to increase the electron-hole wavefunction overlap [14]. And many other efforts have been dedicated to engineer the QW barrier layer [15]–[17] and electron blocking layer (EBL) to achieve better carrier confinement (less carrier leakage) and more uniform carrier distribution (avoiding high carrier density at certain QW) at high current density. For example, Schubert *et al.* used polarization-matched AlGaInN barriers instead of GaN barriers to reduce carrier leakage from the QWs and thus efficiency droop [15]. *Kuo et al.* studied *c*-plane InGaN LEDs with InGaN or GaN-InGaN-GaN barriers that results in favorable carrier injection, uniform carrier distribution and low efficiency droop [16]. It has also been reported that EBL could also affect efficiency droop [18], [19]. Furthermore, devices grown on ternary InGaN substrate also showed improved performance [20]. However, it is difficult to directly alter the QW profile due to the polarization effect of *c*-plane devices because it will make the growth process more complicated and degrade material quality. Recently, growing LED devices on novel nonpolar and semipolar planes of GaN crystals has recently been proposed as a possible solution to suppress the droop effect [21]–[27]. These planes have eliminated or reduced QCSE effect and allow for the growth of thick QWs (up to 12 nm).

To date, highly efficient InGaN LEDs with extremely low efficiency droop have been demonstrated on semipolar ($20\bar{2}\bar{1}$) devices [26][27]. Our previous work in [27] demonstrated a blue-violet ($20\bar{2}\bar{1}$) multiple QWs (MQWs) LEDs with low efficiency droop of 14.3% and pretty high external quantum efficiency (EQE) of 45.3% even at current density 200 A/cm^2, In [27], we fabricated very thick (12 nm) single QW ($20\bar{2}\bar{1}$) LEDs. The EQE (41.2%) only decreased 20% at a current density as high as 400 A/cm^2. This low droop and high efficiency have never been observed on *c*-plane devices. Therefore semipolar ($20\bar{2}\bar{1}$) LEDs are promising to enable efficient high power application of InGaN LEDs and largely reduce power consumption in solid-state lighting and displays. However, the reason for this low droop is still elusive and becoming hot research topics.

Recent studies showed that semipolar ($20\bar{2}\bar{1}$) quantum wells (QWs) have unique properties such as increased indium incorporation rate, polarized emission, and narrow spectrum linewidth [28]–[30], which indicate very different material and optical properties for semipolar ($20\bar{2}\bar{1}$) plane. Despite the encouraging progress on the device side, the physical

Manuscript received October 12, 2015; revised November 16, 2015; accepted January 22, 2016. Date of publication January 25, 2016; date of current version June 15, 2016. This work was supported by Bisgrove Scholar Program from Science Foundation Arizona.

H. Fu, Z. Lu, Y.-H. Zhang and Y. Zhao are with the School of Electrical, Computer, and Energy Engineering, Arizona State University, Tempe, AZ 85287 USA (e-mail: houqiang@asu.edu; zhijian.lv@asu.edu; yhzhang@asu.edu; yuji.zhao@asu.edu).

X.-H. Zhao is with the School of Engineering of Matter, Transport and Energy, Arizona State University, Tempe, AZ 85287 USA (e-mail: xzhao48@asu.edu).

S. P. DenBaars and S. Nakamura are with the Materials Department, University of California, Santa Barbara, CA 93106 USA (e-mail: denbaars@engineering.ucsb.edu; shuji@engineering.ucsb.edu).

Color versions of one or more of the figures in this paper are available online at http://ieeexplore.ieee.org.

Digital Object Identifier 10.1109/JDT.2016.2521618

mechanisms for the low droop performance on (20$\bar{2}\bar{1}$) LEDs are still not well understood. From experimental prospective, although time-resolved photoluminescence (TRPL) has been used to study the decaying properties of InGaN QWs under excitation, systematical comparison of carrier lifetime between c-plane and semipolar LEDs is still lacking. Furthermore no study has linked the carrier lifetime to the droop performance of InGaN LEDs. From theoretical prospective, even though the droop characteristics of c-plane LEDs was very well fitted by conventional *ABC* model, this model was not able to simulate the semipolar LEDs due to its unique low-droop performance. This indicate that a different *ABC* model has to be used for nonpolar and semipolar LEDs where the different physical properties and resulted carrier dynamics must be taken in to account. In this paper, we investigate the emission properties of semipolar (20$\bar{2}\bar{1}$) LEDs using TRPL and steady-state PL measurements, and discuss their influences on the device performances. It is found that the carrier lifetime (radiative and nonradiative lifetime) of semipolar (20$\bar{2}\bar{1}$) InGaN QWs is much smaller than that of the c-plane samples, which may indicate a reduced excess carrier density in semipolar (20$\bar{2}\bar{1}$) LEDs. The smaller radiative carrier lifetime may be expected due to large electron and hole wavefunction overlap in semipolar planes. It can increase the efficiency as well as reduce efficiency droop. However, the role of smaller nonradiative carrier lifetime is twofold: on the one hand, it leads to low efficiency which is unwanted; on the other hand, it can reduce carrier density in the QWs and alleviate the efficiency droop. In the latter sense, nonradiative recombination serves as a beneficial process. Based on experimental results, we propose a modified *ABC* equation with weak phase-space-filling (PSF) effect to model the droop characteristics of semipolar (20$\bar{2}\bar{1}$) LEDs. Very good argument between experimental data and theoretical simulation is obtained.

II. Experiments

Semipolar LEDs were grown by conventional metalorganic chemical vapor deposition (MOCVD) on free-standing (20$\bar{2}\bar{1}$) GaN substrates. The device structure consists of 1 μm Si-doped n-type GaN layer, an InGaN active region, a 20 nm p-type Mg-doped $Al_{0.15}Ga_{0.85}N$ electron blocking layer (EBL), and a 60 nm p-type GaN layer. For comparison, two types of active layer structures were prepared for the semipolar samples: the first group of samples have standard 3 periods of InGaN (3 nm) / GaN (20 nm) multiple QWs (MQWs), while the second group of samples have a 12 nm single QW (SQW) due to the reduced-polarization related effects and flat QW profile. Furthermore, standard c-plane LED samples with 3 periods of InGaN (3 nm) / GaN (20 nm) QWs and otherwise same structures were also prepared as reference. 12 nm InGaN LEDs were however not prepared for c-plane samples due to the large QCSE. LED devices with various wavelengths were prepared for both semipolar (20$\bar{2}\bar{1}$) and c-plane devices, and devices showed comparable light output power.

For experiments, both TRPL and PL measurements are performed on the as-grown samples without encapsulation. Room temperature (300 K) TRPL measurement is carried out using a time-correlated single photon counting (TCSPC) system. The source is an ultrafast titanium-sapphire laser with a 130 fs pulse duration. The output at wavelength of 780 nm is sent through a pulse selector to obtain pulses at a repetition rate of 4 MHz. The pulsed light then goes through a frequency doubler to get 390 nm output light and is incident on the samples. The single photon counting is done by a monochromator, which is set at the peak PL wavelength of the samples, and a high-speed microchannel plate PMT detector. The resolution of this TCSPC setup is about 20 ps. The laser power is 0.1 mW and the beam diameter is about 1 mm. The estimated initial excited carrier density is on the order of 10^{16} cm^{-3} which is very low photogenerated carrier density and hardly affects the internal electric field [31]. Furthermore, PL measurement is performed by a spectrometer equipped with a photomultiplier. The excitation source is 405 nm laser diode. PL data are collected under temperatures of 300 K, 200 K, and 10 K. The laser power density is around 1 W/cm^2. Wavelengths shown in the text and tables below are all PL peak wavelengths of the samples.

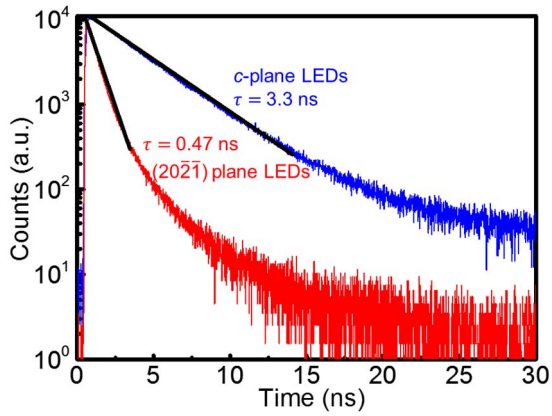

Fig. 1. TRPL spectra of semipolar (20$\bar{2}\bar{1}$) LEDs (red line) and c-plane LEDs (blue line) at room temperature. Carrier lifetime τ is extracted based on exponential decay.

III. Results and Dissicussion

Fig. 1 presents the TRPL measurements of semipolar (20$\bar{2}\bar{1}$) (12 nm SQW) and c-plane samples (3 $\times$ 3 nm MQW) with PL peak wavelength of 436 nm and 455 nm, respectively. The carrier decay dynamics can be simulated using $\Delta n = \Delta n_0 \exp(-t/\tau)$, where Δn is the excess carrier density, Δn_0 is the photogenerated carrier density and τ is the minority carrier lifetime. For semipolar (20$\bar{2}\bar{1}$) LEDs, $\tau = 0.47$ ns; for c-plane LEDs, $\tau = 3.3$ ns. The dominate decay process is likely associated with the exciton emission [32], [33], as the localized carrier emission is widely reported to be the main emitting mechanism in InGaN LEDs [34]. Table I summaries the decay time τ of both semipolar (20$\bar{2}\bar{1}$) samples and c-plane with different wavelength and active layer structures, where the semipolar (20$\bar{2}\bar{1}$) samples showed much smaller τ than c-plane samples. The smaller carrier lifetime of semipolar samples can be due to larger electron-hole wavefuction overlap (smaller τ_{rad})and smaller indium fluctuation (smaller τ_{nonrad})which will be discussed in detail later.

The measured lifetime τ is related to radiative recombination lifetime τ_{rad} and nonradiative recombination lifetime

TABLE I
CARRIER LIFETIMES (τ) OF SEMIPOLAR ($20\bar{2}\bar{1}$) LEDS AND c-PLANE LEDS OBTAINED BY ROOM-TEMPERATURE TRPL MEASUREMENT

Plane	*Active region*	*Wavelength (nm)*	*τ (ns)*
($20\bar{2}\bar{1}$)	12nm SQW	436	0.47
($20\bar{2}\bar{1}$)	12nm SQW	405	0.67
($20\bar{2}\bar{1}$)	3 × 3 nm MQW	452	1.36
($20\bar{2}\bar{1}$)	3 × 3 nm MQW	444	1.70
c-plane	3 × 3 nm MQW	500	3.67
c-plane	3 × 3 nm MQW	455	3.30
c-plane	3 × 3 nm MQW	433	2.80

TABLE II
THE IQES, RADIATIVE LIFETIMES (τ_{rad}), AND NONRADIATIVE LIFETIMES (τ_{nonrad}) OF ($20\bar{2}\bar{1}$) AND C-PLANE INGAN LEDS OBTAINED FROM TEMPERATURE DEPENDENT PL MEASUREMENT

Sample	*Wavelength (nm)*	*IQE ($\eta_{300K/10K}$)*	τ_{rad} *(ns)*	τ_{nonrad} *(ns)*
($20\bar{2}\bar{1}$) 12 nm SQW	436	0.43	1.0	0.8
($20\bar{2}\bar{1}$) 3 × 3 nm MQW	444	0.53	3.2	3.6
c-plane 3 × 3 nm MQW	455	0.54	6.4	7.2

τ_{nonrad} in the equation: $1/\tau = 1/\tau_{rad} + 1/\tau_{nonrad}$. Decomposing the radiative and nonradiative lifetimes can be realized by temperature dependent PL using the equation: $\eta_{300\mathrm{K}/10\mathrm{K}} = \tau_{nonrad}/(\tau_{nonrad} + \tau_{rad})$, where $\eta_{300\mathrm{K}/10\mathrm{K}}$ is the ratio of integrated PL intensity of 300 K to that of 10 K, which is also referred as the internal quantum efficiency (IQE). Temperature-dependent PL is a widely used method to estimate IQE of InGaN LEDs [35]–[37]. At very low temperature (10 K), it's assumed that all the nonradiative recombination centers are frozen and the nonradiative lifetime is regarded as infinite, leading to IQE = 1 at 10 K. Therefore the room temperature IQE is calculated as the ratio of integrated PL intensity of 300 K to that of 10 K [35]–[37]. Figs 2(a) and 2(b) present the temperature-dependent PL results of aforementioned semipolar v and c-plane samples under 300 K, 200 K, and 10 K, respectively. Table II summarizes the obtained IQE, τ_{nonrad}, and τ_{rad} for two semipolar ($20\bar{2}\bar{1}$) samples and one c-plane sample. Both semipolar and c-plane devices showed similar values of IQEs, while the τ_{rad} and τ_{nonrad} on semipolar samples are much smaller than those on the c-plane sample. Smaller τ_{rad} is good both IQE and efficiency droop. While smaller τ_{nonrad} may result in low IQE, it can also alleviate

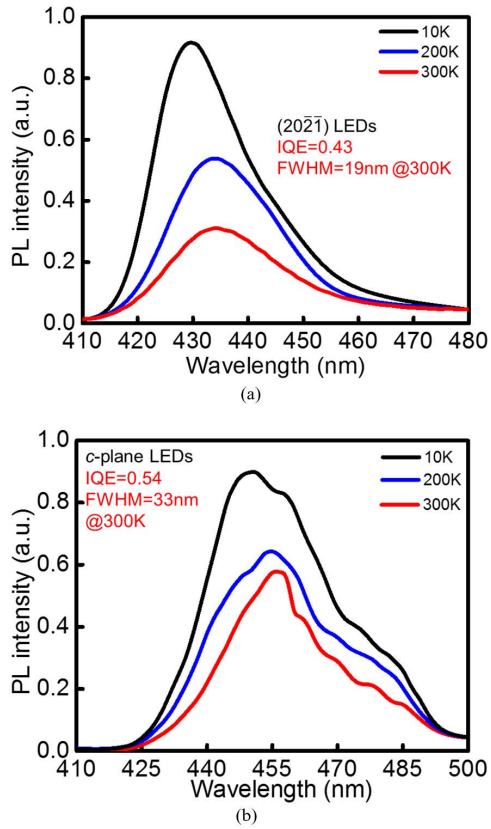

Fig. 2. Steady-state PL spectra of (a) semipolar ($20\bar{2}\bar{1}$) LEDs and (b) c-plane LEDs at 10 K, 200 K and 300 K. IQE is determined by the ratio of integrated intensity of 300 K to 10 K. FWHM at 300 K is also shown.

efficiency droop. Combination of smaller τ_{rad} and τ_{nonrad} gives semipolar LED both high IQE and low efficiency droop. The difference in τ_{rad} can be explained by different QCSE the samples: for c-plane samples, large QCSE exists which decreases the electron and hole's wavefunction overlap, and therefore reduces the recombination rate and increase the radiative lifetime of c-plane samples therefore resulting a larger τ_{rad}. The smaller τ_{nonrad} on semipolar ($20\bar{2}\bar{1}$) samples may be attributed to the smaller indium fluctuation, which will result more carriers trapped in nonradiative recombination centers such as defects. This is further supported by the narrow PL spectra of semipolar ($20\bar{2}\bar{1}$) samples [Fig. 2(a)] in comparison to the broad PL spectra of c-plane samples [Fig. 2(b)]. The full width at half maximum (FWHM) of the semipolar LEDs is 19 nm compared with 33 nm for the c-plane sample. Smaller FWHM is the indicator of more uniform indium distribution in the active region for semipolar LEDs [27]. In addition, we also observed that the carrier lifetime is smaller for 12 nm sample than the 3 × 3 nm sample. This could be attributed to the degraded material quality with increasing QW thickness, which will reduce nonradiative lifetime and therefore lifetime.

The reduced carrier lifetimes (both radiative and nonradiative lifetime) on semipolar ($20\bar{2}\bar{1}$) will have significant impact on the device electro-optical performance. Let's first consider the current density of LEDs. The total injected current density J_{tot} consists of current density due to radiative recombination J_{rad}

and current density due to nonradiative recombination J_{nonrad}. It can be expressed as a function of excess carrier density Δn:

$$J_{tot} = J_{rad} + J_{nonrad} = qd\Delta n(1/\tau_{rad} + 1/\tau_{nonrad}) \quad (1)$$

where q is the carrier charge and d is the active layer thickness. Eq. (1) shows that at the same inject current density J_{tot}, semipolar (20$\bar{2}\bar{1}$) LEDs will have less excess carrier density Δn than c-plane samples due to smaller τ_{rad} and τ_{nonrad}. This may explain the observed low droop performance on semipolar (20$\bar{2}\bar{1}$) LEDs.

In order to verify the correlation between low carrier density and low droop for semipolar (20$\bar{2}\bar{1}$) LEDs, we use a modified *ABC* model to study the droop characteristics on semipolar (20$\bar{2}\bar{1}$) LEDs, where a PSF effect was incorporated into the equation [38], [39]. The equations can be expressed as:

$$J = qd\left(An + \frac{Bn^2}{1+n/n_0} + \frac{Cn^3}{1+n/n_0}\right) \quad (2)$$

$$IQE = \frac{Bn^2}{1+n/n_0} \Big/ \left(An + \frac{Bn^2}{1+n/n_0} + \frac{Cn^3}{1+n/n_0}\right) \quad (3)$$

$$n = \Delta n + N_0 \approx \Delta n \quad (4)$$

where n is the carrier density, N_0 is the doping density, and A, B, C are Shockley-Read-Hall, radiative, and Auger recombination coefficients, respectively. The carrier density n is roughly the value of Δn, as N_0 is much smaller than Δn. A PSF coefficient n_0 is incorporated into the equations. A larger n_0 indicates a weaker PSF effect, and *vice versa*. Physically, the PSF effect stems from Pauli Exclusion Principle, which states that the transition of one electron from valence to a quantum state in conduction band is prohibited if this state is already occupied by an electron. As a result, at high current density, carrier distribution should be described by step-like Fermi-distribution instead of Boltzmann distribution [40]. In the previous studies, it is found that the IQE curve of c-plane devices was very well fitted with the model, the similar n_0 coefficient however was not able to model the semipolar (20$\bar{2}\bar{1}$) LEDs [41]. Here, we propose that at the same injection level, the PSF effect will be much stronger on c-plane LEDs because of higher carrier density. While semipolar (20$\bar{2}\bar{1}$) LEDs, on the other hand, has a weak PSF effect and therefore a larger n_0 should be used in the modeling. Fig. 3(a) presents simulated IQE curves as a function of different current densities, where the n_0 varies from 10^{18} cm^{-3} to 10^{20} cm^{-3}. The A, B, C, and d values used are 2×10^7s^{-1}, 2×10^{-11} cm$^3 \cdot$ s^{-1}, 3×10^{-30} cm$^6 \cdot$ s^{-1} and 18 nm (6 sets of QWs with 3 nm each), respectively, which are typical values used for InGaN LEDs. When n_0 changes, the efficiency curves and associated droop changes dramatically. In Fig. 3(b), we calculated droop ratio of IQE curves with different n_0 at different current density, where droop ratio = $(\mathrm{IQE_{Max}} - \mathrm{IQE_J})/\mathrm{IQE_{Max}} \times 100\%$ ($\mathrm{IQE_{Max}}$ is the IQE maximum and $\mathrm{IQE_J}$ is the IQE at different current densities). It indicates that when n_0 is increased, the droop ratio decreases significantly due to the reduced PSF effect. For example, the IQE curve with $n_0 = 10^{18}$ cm^{-3} shows efficiency droop of 11.7% at 100 A/cm^2 and 38.2% at 400 A/cm^2; however, for $n_0 = 10^{19}$ cm^{-3}, the droop is only 1.7% and 18.7% at 100 A/cm^2 and 400 A/cm^2, respectively. Therefore semipolar (20$\bar{2}\bar{1}$) with smaller carrier density should have weaker PSF effect and smaller efficiency droop, which is simulated and verified using modified *ABC* model later.

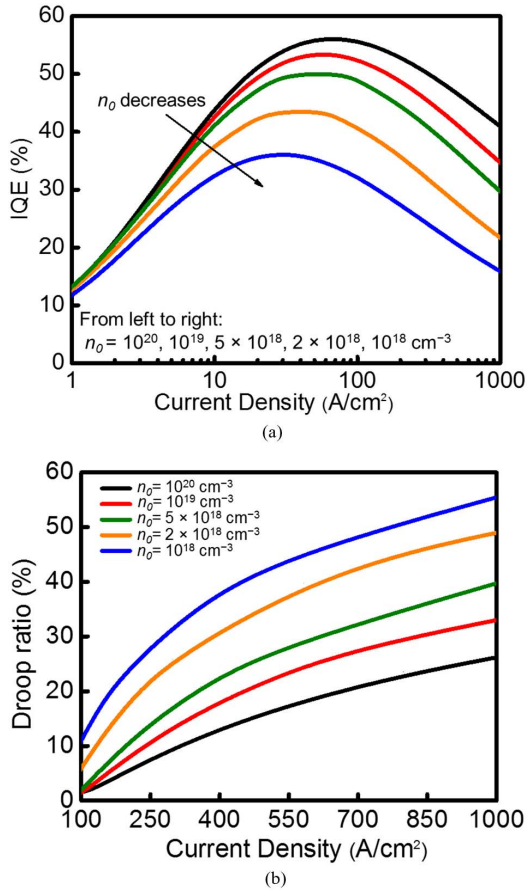

Fig. 3. (a) Calculated IQE curves as a function of current densities using *ABC* model with different n_0 coefficients. (b) Calculated droop ratio of different IQE curves in (a).

Finally, the proposed model with different PSF coefficients n_0 was used to simulate the experimental data of efficiency curve of semipolar (20$\bar{2}\bar{1}$) [27] and c-plane [42] InGaN LEDs, and the results are presented in Fig. 4. It's assumed that the injection efficiency of 100% for both cases and light extraction efficiency of 65% for the semipolar LEDs and 90% for the c-plane LEDs [41], [42]. This assumption is reasonable with current technology status. The IQE curve of c-plane LEDs is well fitted by the model with a strong PSF effect, where $A = 1.6 \times 10^6$s^{-1}, $B = 2.8 \times 10^{-11}$ cm$^3 \cdot$s^{-1}, $C = 4.8 \times 10^{-30}$ cm$^6 \cdot$s^{-1}, $d =$ 15 nm and $n_0 = 1.0 \times 10^{18}$ cm^{-3} were used. However, the IQE curve of semipolar LEDs fits very poorly with strong PSF effect ($n_0 = 1.0 \times 10^{18}$ cm^{-3}) [41]. According to analysis above, a weaker PSF effect exists in semipolar LEDs comparing with c-plane LEDs, and therefore model has to be modified. With a large $n_0 = 5 \times 10^{19}$cm^{-3}, very good agreement between the experimental and fitting data was obtained for semipolar LEDs with $A = 6 \times 10^6$s^{-1}, $B = 5 \times 10^{-11}$ cm$^3 \cdot$s^{-1}, $C = 4.5 \times 10^{-30}$ cm$^6 \cdot$s^{-1}, and $d = 12$ nm. This is consistent with our previous analysis, and *ABC* equation with a weak PSF

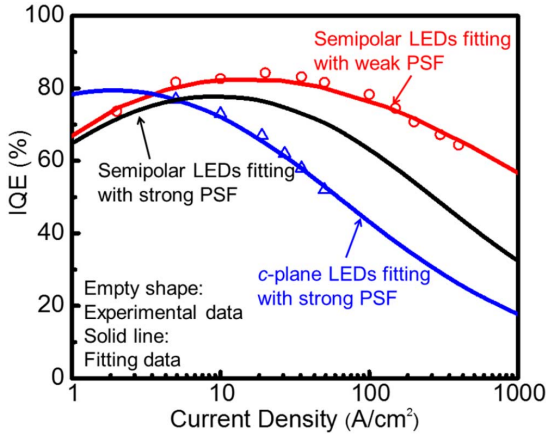

Fig. 4. Simulated IQE curves as a function of current densities for semipolar $(20\bar{2}\bar{1})$ LEDs with weak (red line) and strong (black line) PSF effect, and *c*-plane LEDs with strong PSF effect (blue line). Reported experimental data are also plotted for semipolar $(20\bar{2}\bar{1})$ LEDs [27] (empty triangle) and *c*-plane LEDs [41] (empty circle).

effect shows good agreement with experimental data on semipolar LEDs.

IV. Conclusion

In summary, we studied the emission dynamics of semipolar v InGaN LEDs by TRPL and steady-state PL and the results were discussed. Much smaller carrier lifetimes (radiative and nonradiative carrier lifetime) were obtained from semipolar $(20\bar{2}\bar{1})$ InGaN QWs compared to those on the *c*-plane samples, which indicates a much reduced carrier density on semipolar devices. Based on these results, a modified *ABC* model with weak PSF effect was used to simulate the droop behavior of $(20\bar{2}\bar{1})$ semipolar LEDs, and the simulations showed very good agreement with experimental results. This work suggests a very different emission mechanism and carrier dynamics on semipolar $(20\bar{2}\bar{1})$ LEDs, which may explain the low-droop performance on these devices.

References

[1] S. Nakamura, T. Mukai, and M. Senoh, "Candela-class high-brightness InGaN/AlGaN double-heterostructure blue-light-emitting diodes," *Appl. Phys. Lett.*, vol. 64, p. 1687, 1994.

[2] M. H. Kim, M. F. Schubert, Q. Dai, J. K. Kim, E. F. Schubert, J. Piprek, and Y. Park, "Origin of efficiency droop in GaN-based light-emitting diodes," *Appl. Phys. Lett.*, vol. 91, 2007, Art. ID 183507.

[3] E. Kioupakis, P. Rinke, K. T. Delaney, and C. G. Van de Walle, "Indirect auger recombination as a cause of efficiency droop in nitride light-emitting diodes," *Appl. Phys. Lett.*, vol. 98, 2011, Art. ID 161107.

[4] Y. C. Shen, G. O. Müller, S. Watanabe, N. F. Gardner, A. Munkholm, and M. R. Krames, "Auger recombination in InGaN measured by photoluminescence," *Appl. Phys. Lett.*, vol. 91, 2007, Art. ID 141101.

[5] V. Fiorentini, F. Bernardini, F. Della Sala, A. Di Carlo, and P. Lugli, "Effects of macroscopic polarization in III-V nitride multiple quantum wells," *Phys. Rev. B*, vol. 60, p. 8849, 1999.

[6] S. F. Chichibu, T. Azuhata, M. Sugiyama, T. Kitamura, Y. Ishida, H. Okumura, H. Nakanishi, T. Sota, and T. Mukai, "Optical and structural studies in InGaN quantum well structure laser diodes," *J. Vac. Sci. Technol. B*, vol. 19, p. 2177, 2001.

[7] B. Monemar and E. B. Sernelius, "Defect related issues in the 'current roll-off' in InGaN based light emitting diodes," *Appl. Phys. Lett.*, vol. 91, 2007, Art. ID 181103.

[8] J. Iveland, L. Martinelli, J. Peretti, J. S. Speck, and C. Weisbuch, "Direct measurement of auger electrons emitted from a semiconductor light-emitting diode under electrical injection: Identification of the dominant mechanism for efficiency droop," *Phys. Rev. Lett.*, vol. 110, 2013, Art. ID 177406.

[9] J. Hader, J. V. Moloney, B. Pasenow, S. W. Koch, M. Sabathil, N. Linder, and S. Lutgen, "On the importance of radiative and auger losses in GaN-based quantum wells," *Appl. Phys. Lett.*, vol. 92, 2008, Art. ID 261103.

[10] F. Bertazzi, M. Goano, and E. Bellotti, "A numerical study of Auger recombination in bulk InGaN," *Appl. Phys. Lett.*, vol. 97, 2010, Art. ID 231118.

[11] E. Kioupakis, P. Rinke, K. T. Delaney, and C. G. Van de Walle, "Indriect auger recombination as a cause of efficiency droop in nitride light-emitting diodes," *Appl. Phys. Lett.*, vol. 98, 2011, Art. ID 161107.

[12] H. Y. Ryu, D. S. Shin, and J. I. Shim, "Analysis of efficiency droop in nitride light-emitting diodes by the reduced effective volume of InGaN active material," *Appl. Phys. Lett.*, vol. 100, 2012, Art. ID 131109.

[13] G. B. Lin, D. Meyaard, J. Cho, E. F. Schubert, H. Shim, and C. Sone, "Analytic model for the efficiency droop in semiconductors with asymmetric carrier-transport properties based on drift-induced reduction of injection efficiency," *Appl. Phys. Lett.*, vol. 100, 2012, Art. ID 161106.

[14] H. Zhao, G. Liu, J. Zhang, J. D. Poplawsky, V. Dierolf, and N. Tansu, "Approaches for high internal quantum efficiency green InGaN light-emitting diodes with large overlap quantum wells," *Opt. Exp.*, vol. 19, p. A991, 2011.

[15] M. F. Schubert *et al.*, "Polarization-matched GaInN/AlGaInN multi-quantum-well light-emitting diodes with reduced efficiency droop," *Appl. Phys. Lett.*, vol. 93, 2008, Art. ID 041102.

[16] Y. K. Kuo, T. H. Wang, J. Y. Chang, and M. C. Tsai, "Advantages of InGaN light-emittin diodes with GaN-InGaN-GaN barriers," *Appl. Phys. Lett.*, vol. 99, 2011, Art. ID 091107.

[17] C. C. Pan *et al.*, "High optical power and low efficiency droop blue light-emitting diodes using compositionally step-graded InGaN barrier," *Electron. Lett.*, vol. 51, pp. 1187–1189, 2015.

[18] I. V. Rozhansky and D. A. Zakheim, "Analysis of processes limiting quantum efficiency of AlGaInN LEDs at high pumping," *Phys. Status Solidi A*, vol. 204, p. 227, 2007.

[19] S. Choi *et al.*, "Efficiency droop due to electron spill-over and limited hole injection in III-nitride visible light-emitting diodes employing lattice matched InAlN electron blocking layer," *Appl. Phys. Lett.*, vol. 101, 2012, Art. ID 161110.

[20] J. Zhang and N. Tansu, "Optical gain and laser characteristics of InGaN quantum wells on ternary InGaN substrates," *IEEE Photon. J.*, vol. 5, 2013, Art. ID 2600111.

[21] R. M. Farrell, E. C. Young, F. Wu, S. P. DenBaars, and J. S. Speck, "Materials and growth issues for high-performance nonpolar and semipolar light-emittind devices," *Semicond. Sci. Technol.*, vol. 27, 2012, Art. ID 024001.

[22] D. F. Feezell, J. S. Speck, S. P. DenBaars, and S. Nakamura, "Semipolar $(20\bar{2}\bar{1})$ InGaN/GaN light-emitting diodes for high-efficiency solid-state lighting," *J. Display Technol.*, vol. 9, no. 4, pp. 190–198, Apr. 2013.

[23] P. Walterweit *et al.*, "Nitride semiconductors free of electrostatic fields for efficient white light-emitting diodes," *Nature*, vol. 406, p. 865, 2000.

[24] Y. Zhao *et al.*, "Optimizataion of device structures for bright blue semipolar (1011) light-emitting diodes via metalorganic chemical vapor deposition," *Jpn. J. Appl. Phys.*, vol. 49, 2010, Art. ID 070206.

[25] D. L. Becerra, Y. Zhao, S. H. Oh, C. D. Pynn, K. Fujito, S. P. DenBaars, and S. Nakamura, "High-power low-droop violet semipolar (3031) InGaN/GaN light-emitting diodes with thick active layer design," *Appl. Phys. Lett.*, vol. 105, 2014, Art. ID 171106.

[26] Y. Zhao *et al.*, "High-power blue-violet semipolar $(20\bar{2}\bar{1})$ InGaN/GaN light-emitting diodes with low efficiency droop up at 200 A/cm^2," *Appl. Phys. Express*, vol. 4, 2011, Art. ID 082104.

[27] C. C. Pan *et al.*, "High-power, low-efficiency-droop semipolar $(20\bar{2}\bar{1})$single-quantum-well blue light-emitting diodes," *Appl. Phys. Express*, vol. 5, 2012, Art. ID 062103.

[28] Y. Zhao *et al.*, "Indium incorporation and emission properties of nonpolar and semipolar InGaN quantum wells," *Appl. Phys. Lett.*, vol. 100, 2012, Art. ID 201108.

[29] Y. Zhao *et al.*, "High optical polarization ratio from semipolar $(20\bar{2}\bar{1})$ blue-green InGaN/GaN light-emitting diodes," *Appl. Phys. Lett.*, vol. 99, 2011, Art. ID 051109.

[30] Y. Zhao *et al.*, "Green semipolar $(20\bar{2}\bar{1})$ InGaN light-emitting Diodes with small wavelength shift and narrow spectral linewidth," *Appl. Phys. Exp.*, vol. 6, 2013, Art. ID 062102.

[31] M. Funato *et al.*, "Weak carrier/exciton localization in InGaN quantum wells for green laser diodes fabricated on semipolar $(20\bar{2}\bar{1})$ GaN substrates," *Appl. Phys. Exp.*, vol. 3, 2010, Art. ID 021002.

[32] T. Onuma *et al.*, "Radiative and nonradiative processes in strain-free $Al_xGa_{1-x}N$ films studied by time-resolved photoluminescence and positron annihilation techniques," *J. Appl. Phys.*, vol. 95, p. 2495, 2004.
[33] T. Onuma, Y. Sugiura, T. Yamaguchi, T. Honda, and M. Higashiwaki, "Impacts of AlO_x formation on emission properties of AlN/GaN heterostructures," *Appl. Phys. Exp.*, vol. 8, 2015, Art. ID 052401.
[34] S. F. Chichibu *et al.*, "Origin of defect-insensitive emission probability in In-containing (Al, In, Ga)N alloy semiconductors," *Nat. Mat.*, vol. 5, p. 810, 2006.
[35] D. M. Graham *et al.*, "High photoluminescence quantum efficiency InGaN multiple quantum well structures emitting at 380 nm," *J. Appl. Phys.*, vol. 101, 2007, Art. ID 033516.
[36] D. Zhu *et al.*, "Efficiency measurement of GaN-based quantum well and light-emitting diode strunctrres grown on silicon substrate," *J. Appl. Phys.*, vol. 109, 2011, Art. ID 014502.
[37] S. Deshpande *et al.*, "Formation and nature of InGaN quantum dots in GaN nanowires," *Nano Lett.*, vol. 15, p. 1647, 2015.
[38] A. David and M. J. Grundmann, "Droop in InGaN light-emitting diodes: A differential carrier lifetime analysis," *Appl. Phys. Lett.*, vol. 96, 2010, Art. ID 103504.
[39] H. Fu, Z. Lu, and Y. Zhao, *Phase-space filling effect on the modeling of low-droop performance of semipolar InGaN light-emitting diodes.* unpublished.
[40] J. Hader, J. V. Moloney, and S. W. Koch, "Beyond the ABC: Carrier recombinations in semiconductor lasers," in *Proc. SPIE*, 2006, vol. 6115, p. 61151T.
[41] S. Nakamura and M. R. Krames, "History of gallium–nitride-based light-emitting diodes for illumination," *Proc. IEEE*, vol. 101, no. 10, pp. 2211–2220, Oct. 2013.
[42] K. J. Vampola *et al.*, "Highly efficient broad-area blue and white light-emitting diodes on bulk GaN substrates," *Phys. Stat. Sol. A*, vol. 206, p. 200, 2009.

Houqiang Fu is currently working toward the Ph.D. degree at Arizona State University, Tempe, AZ, USA. His research interests are in the field of optoelectronics, visible light communication, II-V and III-nitride material.

Zhijian Lu is currently working toward the Ph.D. degree at Arizona State University, Tempe, AZ, USA. His research interests are in the field of optoelectronics, visible light communication, II-V and III-nitride material.

Xin-Hao Zhao is currently working toward the Ph.D. degree at Arizona State University, Tempe, AZ, USA. His research interests are in the field of optoelectronics, visible light communication, II-V and III-nitride material.

Yong-Hang Zhang (F'15) received the Doctorate degree in physics from the Max-Planck Institute for Solid States and the University of Stuttgart, Stuttgart, Germany, in 1991. He is currently a Professor of electrical engineering with the School of Electrical, Computer, and Energy Engineering, Arizona State University (ASU), Tempe, AZ, USA. He is also the Associate Dean for Research with Ira Fulton Schools of Engineering and the funding Director of the Center for Photonics Innovation, ASU. He then spent two years with UCSB as an Assistant Research Engineer before he joined Hughes Research Laboratories (HRL) in 1993. He joined ASU in 1996 as an associate professor and was promoted to a professor in 2000. His research interests include molecular beam epitaxy growth, optical properties of semiconductor heterostructures, and optoelectronic devices and their applications.

Steven P. DenBaars (F'05) received the Ph.D. degree in electrical engineering from the University of Southern California, Los Angeles, in 1988. From 1988 to 1991, he was a Member of the technical staff in the Optoelectronics Division, Hewlett-Packard, where he was involved in the growth and fabrication of visible LEDs. He is currently a professor of materials and electrical engineering at the University of California at Santa Barbara. He is also the member of National Academy of Engineering. He has authored or coauthored over 75 technical publications, 60 conference presentation, and holds ten patents. His current research interests are in MOCVD of III–V compound semiconductor materials and devices. Specific research interests include growth of wide-bandgap semiconductors (GaN-based), and their application to blue LED's, lasers, and high-power electronic devices. Dr. DenBaars received the NSF Young Investigator Award in 1994.

Shuji Nakamura was born on May 22, 1954, in Ehime, Japan. He received the B.E., M.S., and Ph.D. degrees in electrical engineering from the University of Tokushima, Japan, in 1977, 1979, and 1994, respectively. He joined Nichia Chemical Industries Ltd., in 1979. In 1988, he spent a year at the University of Florida as a visiting research associate. In 1989, he started the research of blue LEDs using group-III nitride materials. In 1993 and 1995 he developed the first group-III nitride-based blue/green LEDs. He also developed the first group-III nitride-based violet laser diodes (LDs) in 1995. Since 2000, he is a professor of Materials Department of University of California, Santa Barbara, CA, USA. Prof. Nakamura has received a number of awards, including: the Benjamin Franklin Medal Award (2002), the Finnish Millennium Technology Prize (2006), the price of Asturias Award from Spain (2008) and the Harvey Prize of Israel Institute of Technology (2010). He is also the member of National Academy of Engineering. He was awarded the Nobel Prize in physics in 2014.

Yuji Zhao received the B.S. degree in Microelectronics from Fudan University, China in 2008, and the Ph.D degree in Electrical and Computer Engineering from University of California, Santa Barbara (UCSB) in 2012, after Nobel Laureate Professor Shuji Nakamura. Prior to joining ASU in 2014, he was an Assistant Project Scientist in the Materials Department and Solid State Lighting and Energy Center (SSLEC) at UCSB. He is an assistant professor at ASU. His research focus on advanced electronic and optoelectronic devices based on new materials, currently wide bandgap III-nitride semiconductors.